RSC Advances

PAPER

View Article Online
View Journal | View Issue

Cite this: *RSC Adv.*, 2015, **5**, 12434

# Microstructural transition of aqueous CTAB micelles in the presence of long chain alcohols

Jasila Karayil,[a] Sanjeev Kumar,[b] P. A. Hassan,[c] Yeshayahu Talmon[d] and Lisa Sreejith*[a]

The effect of long chain alcohols ($C_9OH$–$C_{12}OH$) on the micellar properties of CTAB in the presence of an inorganic salt, KBr, has been systematically studied by viscometry, rheology, DLS and the direct imaging technique, *i.e.* cryo-TEM. The molar ratio of CTAB/KBr was fixed at 1 : 1 and the alcohol concentration ranged from 0.005 to 0.03 M. With an increase in concentration of the alcohol, the Mitchell–Ninham surfactant parameter, $R_p$, increases, which favours micellar growth. The viscosity results showed a maxima followed by a drop (regions I–III). In region I, the samples were less viscous and have a propensity to form short cylindrical micelles. The rheological response of the samples in the plateau region (region II) showed strong viscoelasticity, indicating the presence of worm-like micelles, which was confirmed by cryo-TEM and DLS analysis. A drop in viscosity (region III) was observed at higher concentrations of alcohol. The observed increase in the apparent hydrodynamic diameter of the micelles with the concentration of alcohol confirmed the alcohol induced micelle growth. An unusual temperature response was another feature noticed for the $C_9OH$ samples in region III, and the cryo-TEM investigation revealed the presence of vesicles, which are nearly absent in $C_{10}$–$C_{12}OH$. Therefore, the results suggest a strong dependence of the surfactant morphology on the solubilisation site of the added alcohol, which could be further affected by temperature.

Received 9th September 2014
Accepted 15th December 2014

DOI: 10.1039/c4ra10052b

www.rsc.org/advances

## Introduction

The self-assembly of surfactant molecules utilizes non-covalent interactions such as hydrophobic, van der Waals, hydration and electrostatic interactions.[1–3] The microstructure of the self-assembly can be correlated to the Mitchell–Ninham parameters, $R_p$,[4] which depend upon the effective ratio of volume ($v$) and the length ($l$) of the alkyl tail part to the head group area ($a_o$) for a typical surfactant ($R_p = v/a_o l$). Fang and Venable used $R_p$ to explain a series of structural transitions.[5] The size and shape of the micelle were found to affect the counter-ion condensation in the micellar head group region.[8] Inorganic and organic counterions were reported to induce micellar growth due to the screening of the electrostatic repulsion between the head groups (decrease in $a_o$ and hence increase in $R_p$).[6,7] The partitioning of organic additives into head group region can also modify the inter-head group repulsion together with an increase in $v$, leading to an increase in $R_p$.[9] This increase in $R_p$ facilitates the formation of various morphologies consistent with the geometrical packing model of Israelachvili *et al.*[10]

Extensive work has been carried out on the effect of different additives on the micellar morphologies.[11–14] Alcohols are one of the widely used additives added to a surfactant to form microemulsions.[15] Depending upon the hydrophobicity of the alcohol, the added alcohol can locate/partition either on the micellar surface, palisade layer and/or core (Fig. 1). The locus of the alcohol solubilisation in the micelle is the main factor that determines its action on a surfactant system.[16] The effect of short and medium chain alcohols on the micellar growth of ionic micelles has been investigated using a variety of techniques.[17–20] It was noticed that short chain alcohols ($n < 3$) tend to remain in the aqueous phase, alter the hydrogen-bonding structure of water, and thereby disrupt the micelles and decrease the hydrodynamic diameter of the micelles.[21] The aforementioned behaviour was reported recently by Taliha *et al.*[22] They found that the addition of ($C_1OH$ to

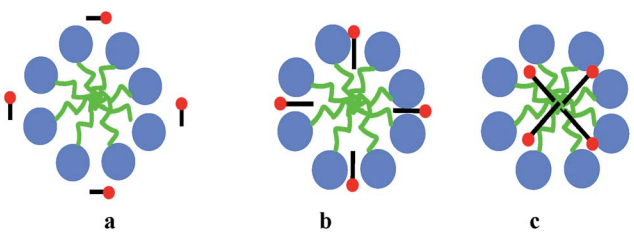


Fig. 1 Schematics of location of the solubilisation of alcohols: (a) near the micellar surface (b) in the palisade region and (c) in the micellar core is an alcohol of different chain length.

[a]*Department of Chemistry, NIT Calicut, Kerala, India. E-mail: jessekarayil@gmail.com; lisa@nitc.ac.in; Fax: +91-495-22867280; Tel: +91-495-2286553*

[b]*Department of Applied Chemistry, Faculty of Technology and Engineering, The Maharaja Sayajirao University of Baroda, Vadodara, India*

[c]*Chemistry Division, BARC, Mumbai, India*

[d]*Department of Chemical Engineering, Technion-Israel Institute of Technology, Haifa, Israel*

$C_3OH$) to a micellar solution leads to an increase in CMC and are less effective in inducing micellar growth in cationic surfactants. Medium chain alcohols ($n > 4$) were found to intercalate between micelles (palisade layer) causing a decrease in CMC and thereby promotes micelle growth.[23–26] Kuperkar and his co-workers[27] examined the effect of linear alcohols ($C_2OH$ to $C_6OH$) on cationic surfactants and emphasised that upon increasing the hydrocarbon chain length of alcohol ($n$) there is a marked decrease in CMC, resulting in pronounced micellar growth. Similar behaviour was reported for an ionic micellar system with alcohol chain length up to $C_8$.[14] Thus depending upon their carbon chain length ($n$), alcohols can act as either a co-solvent or a co-surfactant.

It is a well-established fact that an inorganic salt can enhance the effect of additives on the self-assembling nature of a surfactant. David *et al.*[28] studied the synergistic effect of salt and alcohol on cationic surfactants and reported an enhancement of viscosity in the system. Added salt may affect the partitioning of alcohol between the micelle and aqueous phase.[29] It is thus of great interest to see how an additive at different micellar solubilisation sites can influence the association morphology and its subsequent physical properties. It would then be easier to mimic more complex biological systems since they involve hydrophobic interactions like simple surfactant morphologies (micelles or vesicles).[30–32]

There are only a few reports on the study of micellar transitions of CTAB in the presence of long chain alcohols. Recently, we have initiated a study on the micelle to vesicle transition (MVT) in a CTAB/*n*-octanol/KBr system.[33] Furthermore, a neutron scattering study showed that disk-like aggregates are present in a potassium dodecanoate–dodecanol–water system. It is expected that a higher chain length alcohol can only be solubilised in either the micellar palisade layer or in the core and can potentially increase the $R_p$ at relatively low concentrations, as they are nearly insoluble in the micellar background aqueous solution. Therefore, a higher chain length alcohol can be the appropriate candidate to tune $R_p$.

The abovementioned facts prompted us to carry out a systematic study on CTAB/KBr in the presence of higher homologues of alcohols. This paper is the first ever report of the combined effect of long chain alcohols ($C_9OH$–$C_{12}OH$) and KBr on the structural transition of CTAB using viscosity, rheology, DLS and cryo-TEM techniques. We also monitored the viscosity behaviour of the above systems as a function of temperature ranging from 25–60 °C. A few systems showed pronounced viscosification on heating. Such thermo-responsive structural transitions have been previously reported only for a few systems.[33–35] A heating induced viscosity increase can be of great importance in various biological and mechanical applications (microfluidic devices and hydraulic fracturing).[36–38] Therefore, the material studied in the present study may have great potential for some of these applications.

# Experimental sections

### Materials

CTAB (Merck Germany, 99% assay) was purchased and used as received. All the additives, *i.e.* KBr (Himedia, 99% assay), *n*-nonanol (Merck, 99% assay), *n*-decanol (Merck, 99% assay), *n*-undecanol (Merck, 99% assay) and *n*-dodecanol (Merck, 99% assay) were of high purity and used without further purification. The sample solutions were prepared in Millipore water with resistivity of 18.2 MΩ cm.

### Sample preparation

The stock solution was prepared by dissolving a weighed amount of CTAB and KBr in Millipore water. The alcohols at various concentrations were added to this solution using a glass microsyringe (Hamilton) and heated to 50 °C under continuous stirring for half an hour until the solution became homogeneous. The samples were then kept at room temperature for at least one day to attain equilibrium.

### Rheology

Steady and dynamic rheological experiments were performed on a controlled stress rheometer (Anton Paar Physica MCR-301) with a parallel plate sensor (50 mm diameter), and the gap was 1 mm. Experiments were performed at 30 ± 0.01 °C, and the viscosity of the sample was obtained from steady-shear measurements with the shear rate ranging from 0.3 to 500 $s^{-1}$. Frequency sweep measurements were performed at a given stress in the frequency region varying from 0.1 to 100 rad $s^{-1}$. The samples were equilibrated at least 15 minutes at the measuring temperature prior to obtaining the experimental measurement.

### Viscosity measurements

The absolute viscosity of the samples under conditions of defined shear rate and shear stress were determined using a programmable Brookfield DV – II + cone and plate viscometer (Brookfield Engineering Laboratories, Inc – USA) thermostated at a temperature range of 25–60 ± 1 °C. Prior to the measurement samples were mounted for at least 30 minutes to attain thermal equilibrium.

### DLS measurements

Measurements were performed with a Malvern 4800 Autosizer employing a 7132 digital correlator at a scattering angle of 130°. A vertically polarized light of wavelength 514.5 nm from an argon laser was used as the incident beam. All solutions were filtered with a 0.2 m membrane filter before the measurements to avoid interference from dust. The measured intensity correlation functions were analyzed using the method of cumulants[33] where the unimodal distribution of relaxation time is considered. The size distribution was obtained using the CONTIN algorithm wherever needed.

### Cryo TEM

Vitrified cryo-TEM specimens were prepared in a controlled environment vitrification system (CEVS) at 25 °C and 100% relative humidity to avoid loss of volatiles, followed by quenching into liquid ethane at its freezing point. The specimens, kept below −178 °C, were examined using a FEI T12 G2

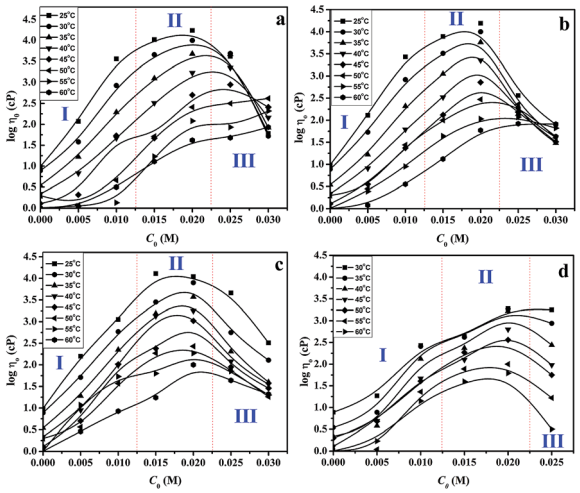


Fig. 2 The effect of alcohol concentration ($C_0$) on the zero shear viscosity, log(cP) of 0.1 M CTAB/0.1 M KBr for (a) nonanol, (b) decanol, (c) undecanol and (d) dodecanol at temperatures ranging from 25 to 60 °C.

transmission electron microscope operated at 120 kV equipped with a Gatan 626 cryo-holder system. Images were recorded digitally on a Gatan US1000 high-resolution cooled-CCD camera using Digital Micrograph 3.4 software package in the low dose imaging mode.

## Results and discussion

### The effect of concentration and the chain length of alcohol on the CTAB/KBr micellar system

Mukerjee[39] pointed out that if an additive is surface active to a hydrocarbon–water interface, it will solubilise in the head group region (Fig. 1b) and may promote structural transitions. Greater partitioning of the additive to the interior (Fig. 1c) was shown to reduce micellar growth by virtue of releasing the requirement of the monomer tails to reach the centre of the micelles and therefore will swell.[40,41] Spherical micelles ($R_P < 1/3$) were found to be less viscous, whereas the worm-like micelles ($1/3 < R_P < 1/2$) showed pronounced viscosity. Hence, viscosity results provide an indication of the structural transitions and can be used to study the morphological evolution in a solution of surfactant.[42]

The 0.1 M CTAB/0.1 M KBr micellar solution was noted to be less viscous (≈10 cP) and has a propensity to form spherical (or short rod-shaped) micelles. However, the addition of long chain alcohol to 0.1 M CTAB/0.1 M KBr micellar solution dramatically increases its viscosity (≈17 500 cP). The zero shear viscosity ($\eta_0$) of aqueous 0.1 M CTAB/0.1 M KBr with varying concentration of $C_9OH$–$C_{12}OH$ at different temperatures (25–60 °C) is shown in Fig. 2(a–d) and it was observed that $\eta_0$ is a strong function of concentration ($C_0$) and chain length ($n$) of alcohol (peaked behaviour). Three regions (region I–III) were identified and they were explained on the basis of the formation of ordered structures/phase behaviour. At lower $C_0$ (<0.01 M), the viscosity increases distinctly, which corresponds to micellar elongation (region I). With an increase in $C_0$, these micelles can grow anisotropically into cylindrical ones and at the critical $C_0$, they entangle to form a network of worm-like micelles with a rapid increase in viscosity, $\eta_0^{max}$ (region II). This $C_0$, at which the viscosity increases sharply, can be considered to be the concentration needed for a sphere to rod transition (s → r).

Desai *et al.*[43] have studied the (s → r) of CTAB in the presence of *n*-octanol and proposed that octanol forms alcohol–surfactant mixed micelles, reduces the repulsion between the charged head groups, and therefore modifies the effective $R_p$ and is responsible for micelle growth. When alcohol molecules are solubilised in the micellar palisade layer (Fig. 1b), they will contribute towards the overall volume of a micelle; therefore, volume per surfactant monomer will effectively increase and is responsible for an increase in $R_p$. A similar analogy can be extended to the other long chain alcohols used here and was believed to cause micellar growth due to a decrease in the electrostatic repulsion by the addition of KBr and an increase in the hydrophobic interactions by intercalation of the alcohol molecules between monomers of the micelle (as $R_p$ will also increase as mentioned above). On further addition of alcohol, the samples become less viscous and showed a bluish hue (region III). The bluish colour is a manifestation of the Tyndall effect, due to the presence of scatterers in solution and is generally seen for solutions containing vesicles.[44]

To better understand the rich variation in viscosity, we have performed rheological measurements with selected samples at 30 °C. The steady shear viscosities obtained for the samples (≥0.01 M $C_0$) showed non-Newtonian behaviour (Fig. 3), *i.e.*, the viscosity decreases drastically with an increase in the shear rate (shear thinning behaviour). Upon increasing the concentration of alcohol the viscosity increases promptly, an indication of the formation of rigid rods of medium length, which slowly converts into flexible worm-like micelles.[45,46] Here the samples are clear and viscoelastic; however, at higher $C_0$ (0.03 M), shear thinning becomes less prominent (deviation from non-

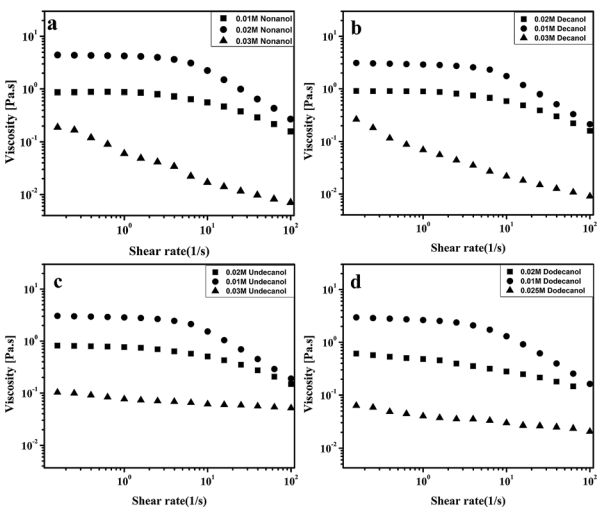


Fig. 3 The steady shear rheological response of 0.1 M CTAB/0.1 M KBr as a function of $C_0$: (a) nonanol, (b) decanol, (c) undecanol and (d) dodecanol. ■ is 0.01 M, ● is 0.02 M, and ▲ is 0.03 M alcohol.

Newtonian behaviour). Note that the non-viscous and bluish nature of the sample solution reflects the presence of unilamellar vesicles. Vesicular dispersion was expected to be dilute and therefore nearly Newtonian behaviour without much variation in viscosity was observed.[47,48] A similar vesicular phase with *n*-decanol in sodium *N*-lauroylsarcosinate hydrate has already been reported.[49]

The viscoelastic properties of the samples were analyzed by oscillatory-shear experiments. The variation of elastic modulus ($G'$) and viscous modulus ($G''$) as a function of frequency ($\omega$) at 30 °C are given in Fig. 4.

The dynamic rheological response of the samples shows that at high frequencies it behaves elastically ($G' > G''$); however, at low frequencies, it switches to a viscous behaviour ($G'' > G'$), a typical viscoelastic behaviour shown by worm-like micellar solutions.[9] The rheological behaviour of this system was characterized by the generalized Maxwell model. For a Maxwell fluid, the variation of the $G'$ and $G''$ can be given as follows:[50,51]

$$G'(\omega) = \frac{\omega^2\tau^2}{1+(\omega\tau)^2}G_0$$

$$G''(\omega) = \frac{\omega\tau}{1+(\omega\tau)^2}G_0$$

where $\omega$ is the frequency, $G_0$ is the plateau modulus and $\tau$ the relaxation time. At a lower frequency, Maxwell behaviour with a single relaxation time was observed for the samples and the data fits reasonably well in the Maxwell model. This behaviour in the low-frequency regime for viscoelastic fluids is usually demonstrated in a Cole–Cole plot of $G'$ *vs.* $G''$ (Fig. 5). A semicircular relationship over the majority of frequencies was noted for a Maxwell fluid.[51,52] The deviation of $G''$ from the Maxwell model in the higher frequency region is another characteristic feature of worm-like micelles. This observation corresponds to the fact that the worm-like micelles are in dynamic equilibrium and there is a rapid breaking and recombination process (shown by living polymers).[53] This is related to breathing or Rouse-like motion.[54]

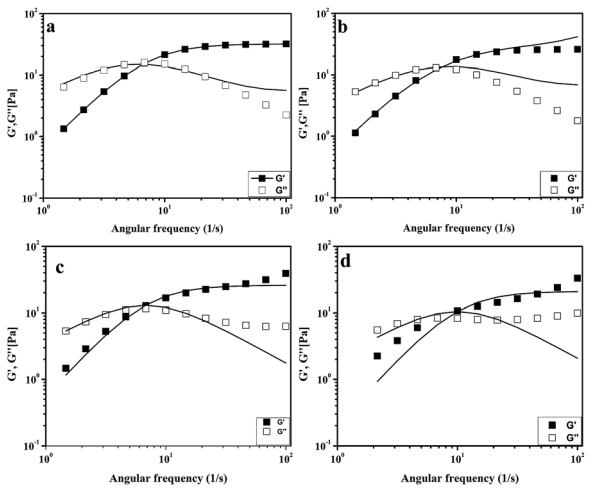


Fig. 4 Dynamic rheological response of $G'$ (closed) and $G''$ (open) for 0.1 M CTAB/0.1 M KBr at $C_0$ 0.02 M: (a) nonanol, (b) decanol, (c) undecanol and (d) dodecanol at 30 °C.

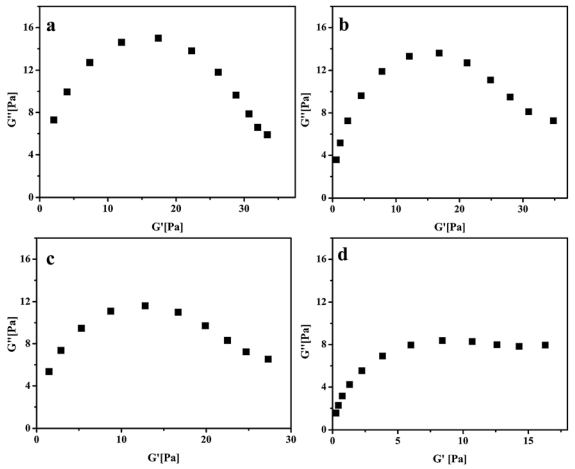


Fig. 5 The Cole–Cole plot for worm-like micellar solutions of 0.1 M CTAB/0.1 M KBr at $C_0$ (0.02 M): (a) nonanol, (b) decanol, (c) undecanol and (d) dodecanol at 30 °C.

Shear plateau in worm-like micelles have been widely observed in the literature. Above a characteristic shear rate, the flow curve shows a plateau with a finite slope.[55,56] The nature of this behaviour as well as the mechanism at its origin is still the subject of intense debate. Cates *et al.*[57] have proposed that the plateau is a signature of mechanical instability in the form of shear bands. Fig. 6 shows the flow curve for 0.1 M CTAB/0.1 M KBr containing 0.02 M $C_9OH$–$C_{12}OH$ at 30 °C. The flow curve exhibits a discontinuity of the slope at the critical value, followed by a stress plateau, which persists over decades in strain rates. This further confirms the presence of worm-like micelles in the systems.

The hydrophobic interactions between the embedded alcohol and hydrocarbon part of micelles causes a reduction in the free energy of the micelles and can promote its growth. As a result, the viscosity of system increases with an increase in chain length. An increase in viscosity upon increasing the chain length of the alcohol ($n$) from 9 to 12 was expected. However,

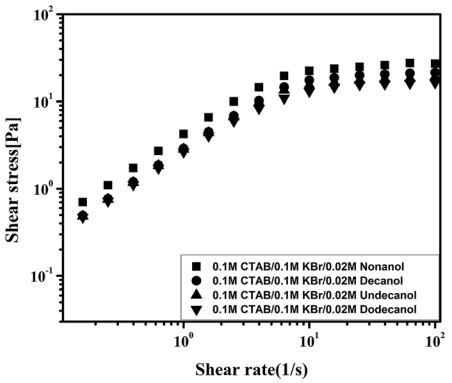


Fig. 6 Shear stress as a function of the shear rate for 0.1 M CTAB/0.1 M KBr/0.02 M $C_9OH$–$C_{12}OH$ at 30 °C.

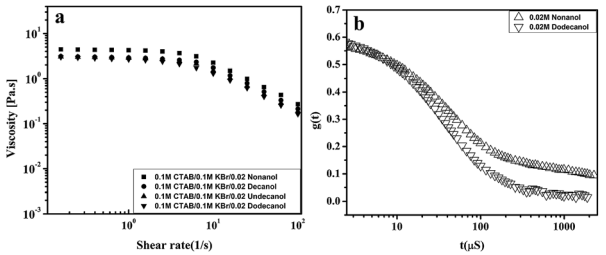


Fig. 7 (a) The Shear viscosity of 0.1 M CTAB/0.1 M KBr/0.02 M $C_9OH$–$C_{12}OH$ at 30 °C. (b) Variation of the electric field correlation function with time for 0.02 M $C_9OH$ and $C_{12}OH$.

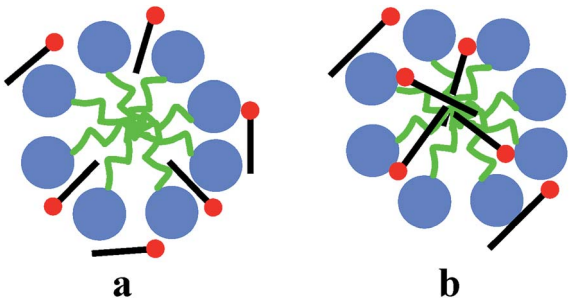


Fig. 8 Schematic diagram for the proposed solubilisation site of nonanol and dodecanol in CTAB micelles.

steady-shear rheological data for the samples (Fig. 6) shows that there is viscosity drop from nonanol to dodecanol. The zero shear viscosity of the CTAB/KBr/nonanol system is 5 times higher than CTAB/KBr/dodecanol system (Fig.7a). Moreover, the average relaxation time of CTAB/KBr/nonanol was greater than the CTAB/KBr/dodecanol system (Fig. 7b). This could be due to the deeper penetration of dodecanol in the CTAB micellar core (Fig. 8). Therefore, the effectiveness of dodecanol to induce micellar growth diminishes since core solubilisation fails to cause much growth.

DLS was employed to track the hydrodynamic diameter of the microstructures. DLS data for the 0.1 M CTAB + 0.1 M KBr system shows a low hydrodynamic diameter in the absence of alcohol and is consistent with low viscosity as shown in Fig. 2. With an increase in concentration of alcohol, the average hydrodynamic diameter of the micelle shifts to the larger diameter region (Fig. 9).

Fig. 10 shows the variation of the electric field correlation function in the presence of an increasing concentration of alcohol. It was observed that the correlation function shifts to a longer time upon increasing the concentration of alcohol. This indicates an increase in the average relaxation time with an increase in the concentration of alcohol, suggesting an increase in the average dimension of the micelles (micellar elongation).

Direct imaging cryo-TEM correlates the presented data with the microstructure of the micelles shown in different regions of Fig. 1. Cryo-TEM examination of the samples in region II shows the presence of an entangled network of worms with branching (Fig. 11). These worm-like micelles impart high viscosity to the

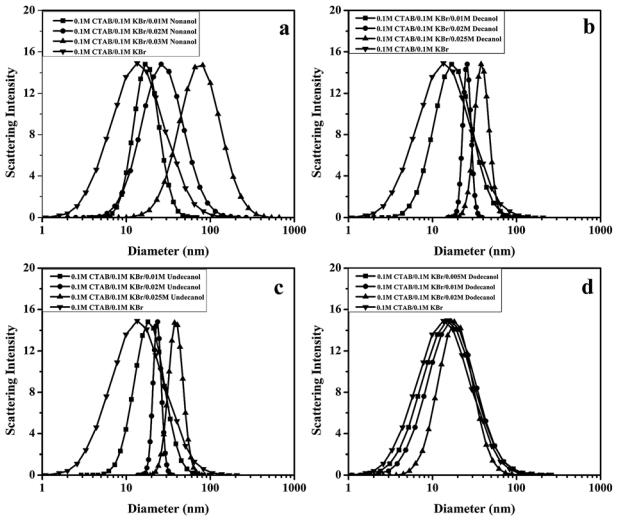


Fig. 9 Intensity weighted distribution of apparent hydrodynamic diameter of 0.1 M CTAB/0.1 M KBr micellar solutions as a function of $C_0$: (a) nonanol, (b) decanol, (c) undecanol and (d) dodecanol.

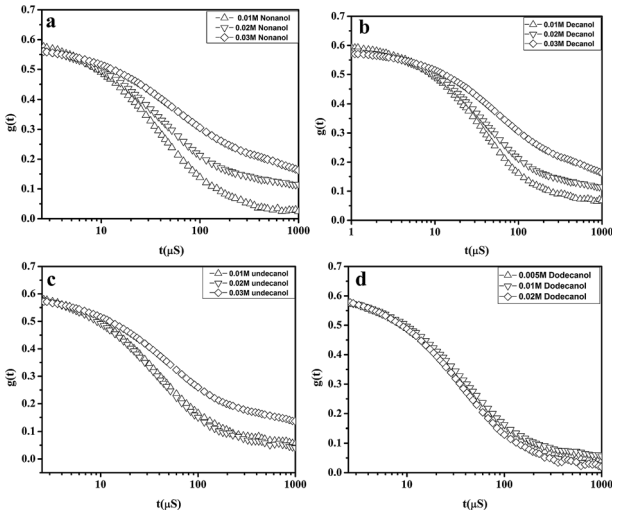


Fig. 10 Variation of the electric field correlation function with time for 0.1 M CTAB/0.1 M KBr solution as a function of $C_0$: (a) nonanol, (b) decanol, (c) undecanol and (d) dodecanol.

system and the solution becomes viscoelastic as observed in region II of Fig. 2 and by the rheological studies (Fig. 4).

The Cryo-TEM images (Fig. 12) for samples from region III ($C_0$ = 0.03 M) depict the coexistence of worm-like micelles (arrow-1), unilamellar vesicles (arrow-2) and oligovesicles (arrow 3). To our surprise, the worm-like micelle to vesicle transition was found only with the additive nonanol (Fig. 12a and b). This exclusive ability of nonanol to transform rod-shaped micelles to vesicles is a complicated question to answer. A plausible explanation may be the distribution of nonanol between the head group region and micellar core. Such distribution may impart flexibility to the aggregate to transform from the rod-shape micelle to a vesicle. It is expected that after the initial addition of nonanol, it may partition more in the

 

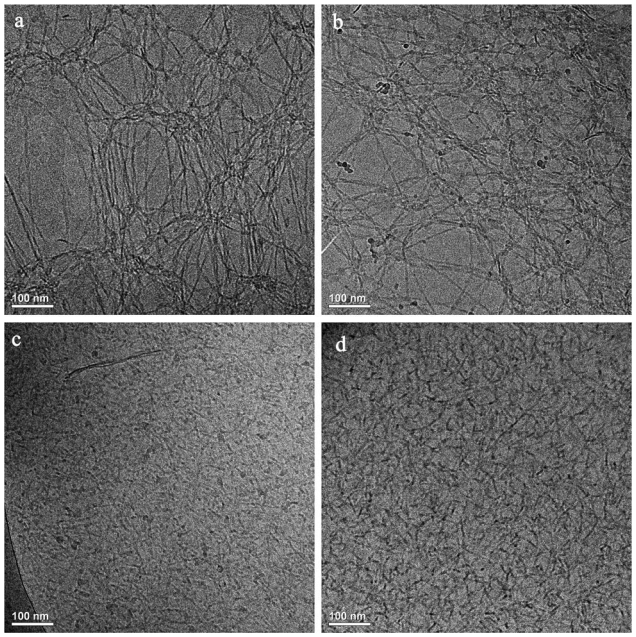


Fig. 11 Cryo-TEM micrographs of the worm-like micelles formed in 0.1 M CTAB/0.1 M KBr at $C_0$ (0.02 M): (a) nonanol, (b) decanol, (c) undecanol and (d) dodecanol. Scale bar 100 nm.

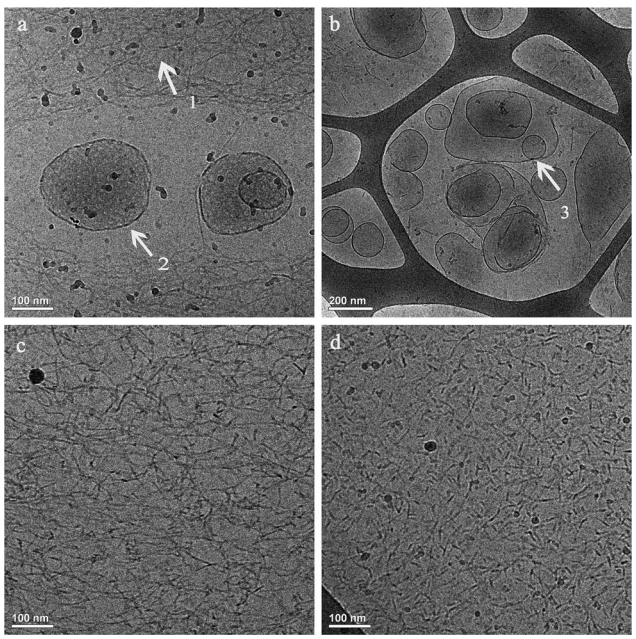


Fig. 12 Cryo-TEM micrographs of samples located above the peak viscosity region $C_0$ 0.03 M nonanol at (a) scale bar 100 and (b) 200 nm. The coexistence of thread-like micelles (arrow-1), unilamellar vesicles (arrow-2) and oligo vesicles (arrow 3) can be seen. Elongated and short rod-like micelles are the dominant microstructures for (c) 0.03 M Decanol and (d) 0.03 M undecanol.

micellar head group region, which is responsible for the formation of rod- or worm-like micelles. However, at higher concentrations, one can expect nonanol partitioning towards the interior or the core of the micelle. These two partitioning sites (head group and interior regions) may be responsible for the above transition. The values of the vesicular size obtained in the micrographs were in agreement with those obtained by other scientists who have investigated similar mixed micelle systems.[58,59] The other alcohol ($C_{10}$OH and $C_{11}$OH) incorporated samples at higher concentrations causes a breakdown of the worm-like micelles to short cylinders as is clear from the corresponding cryo-TEM images (Fig. 12c and d). This behaviour can be explained in light of the increased hydrophobicity of higher chain length alcohols, which force the additives to go into the micelle core. In this situation, the structure/flexibility of the head group region would be affected. It has been reported that head group partitioning would always be responsible for micellar growth while interior solubilisation causes lower order aggregates. This indeed was observed in the case of $C_{10}$OH and $C_{11}$OH (Fig. 12c and d).

### The effect of temperature

The behaviour of worm-like micelles greatly depends on temperature. The Arrhenius plot of log $\eta_0$ *vs.* $1/T$ (where $T$ is the absolute temperature) falls on a straight line (Fig. 13), the slope of which yields the flow activation energy ($E_a$). The values of $E_a$ ranging from 70 to 300 kJ mol$^{-1}$ have been reported for various micellar solutions.[60] $\eta_0$ decreases with a rise in temperature, showing that it decays exponentially with temperature. This exponential decay of viscosity with temperature is in accordance with the Arrhenius type of equation for worm-like micelles:[61]

$$\eta_0 = A\mathrm{e}^{-E_a/RT}$$

where $R$ is the universal gas constant and $A$ is Arrhenius constant.

The values of flow activation energies were determined from the slopes of the straight lines and calculated to be 105, 102, 96 and 80 kJ mol$^{-1}$ for $C_9$OH to $C_{12}$OH, respectively. These values are comparable to the reported value (70–300 kJ mol$^{-1}$) for worm-like micelles obtained in other systems. It should be

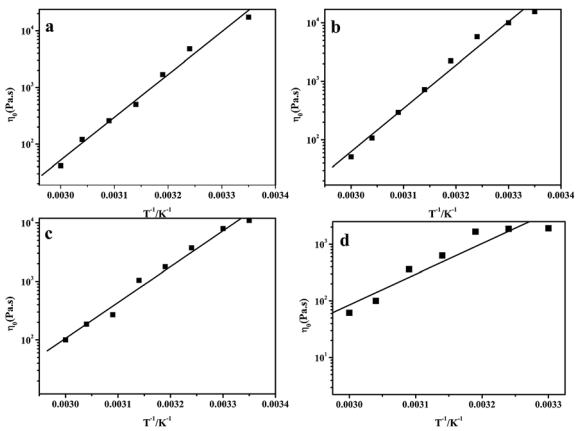


Fig. 13 The effect of temperature on the zero-shear viscosity ($\eta_0$) *versus* $1/T$ on a semilog scale for 0.1 M CTAB/0.1 M KBr systems at $C_0$ (0.02 M): (a) nonanol, (b) decanol, (c) undecanol (d) and dodecanol. Solid lines are the fits to the data point.

noted that CTAB/KBr/Dodecanol system shows a large deviation from the straight line, which shows that it is least viscoelastic among the other three systems. However, the $E_a$ values also support the formation of longer micelles as observed by the other experimental data (viscometry, DLS and cryo-TEM).

An unusual thermo viscosification was observed for CTAB/KBr/0.03 M nonanol system. This micellar solution consists of vesicles, as demonstrated by cryo-TEM. However, upon increasing the temperature, there is substantial increase in viscosity (~7 fold increase) and the sample turns into an optically clear, viscous fluid. This was attributed to a micellar shape transition upon heating. Probably, a vesicle to rod-like transition takes place with temperature. At higher temperature, some of the nonanol molecules may leach out from the micellar interior to the surface region, thereby decreasing the $R_p$ and modify the morphology to rod-like with a concomitant increase in viscosity (Fig. 2a, region III).

## Conclusions

Cetyl trimethyl ammonium bromide in the presence of additives (KBr and long chain alcohols) can show various microstructural transitions. We demonstrated that a small rod-like to worm-like to vesicle transformation of aggregates takes place with a continuous increase in the concentration of alcohol. These transitions take place within a narrow concentration range of alcohol (0.01–0.03 M). DLS data were complementary to the viscosity and rheological data and support the micellar growth. Cryo-TEM data shows the spontaneous formation of unilamellar, multilamellar, and oligovesicles in the 0.03 M nonanol system. However, such rich morphological changes were absent with higher chain length alcohols. On combining the present results of nonanol with our previous study,[33] it can be concluded that alcohols with a chain length ($n = 8$ or 9) produces vesicles. Furthermore, the effectiveness of an additive to modify the $R_p$ value determines the overall morphology at a particular concentration.

## Acknowledgements

We would like to acknowledge Dr Ellina Kesselman and Dr Judith Schmidt (Technion-Israel Institute of Technology) for their help in the Cryo-TEM analysis, Dr B.V.R. Tata, Head, Light Scattering Studies Section, Condensed Matter Physics Division, Indira Gandhi Centre for Atomic Research, Kalpakkam, India for permitting us to carry out rheological experiments. The research grant from UGC as a fellowship (19-12/2010(i) EU-IV) is also acknowledged.

## Notes and references

1 D. Chandler, *Nature*, 2005, **437**, 640.
2 C. B. Minkenberg, L. Florusse, R. Eelkema, G. J. M. Koper and J. V. VanEsch, *J. Am. Chem. Soc.*, 2009, **11**, 11274.
3 S. Kumar, A. Bhadoria, H. Patel and V. K. Aswal, *J. Phys. Chem. B*, 2012, **116**, 3699.
4 D. J. Mitchell and B. W. Ninham, *J. Chem. Soc., Faraday Trans. 2*, 1981, **77**, 601.
5 J. Fang and R. L. Venable, *J. Colloid Interface Sci.*, 1987, **117**, 448.
6 H. Rehage and H. Hoffman, *Mol. Phys.*, 1991, **74**, 933.
7 R. T. Buwalda, M. C. A. Stuart and J. F. B. Engberts, *Langmuir*, 2000, **16**, 6780.
8 V. K. Aswal and P. S. Goyal, *Phys. Rev.*, 2000, **61**, 2947.
9 Z. Lin, J. J. Cai, L. E. Scriven and H. T. Davis, *J. Phys. Chem.*, 1994, **98**, 5984.
10 J. N. Israelachvili, D. J. Mitchell and B. W. Ninham, *J. Chem. Soc., Faraday Trans. 1*, 1977, **72**, 1525.
11 S. Kumar, D. Sharma, G. Ghosh and Kabir-ud-Din, *Langmuir*, 2005, **21**, 9446.
12 N. Vlachy, M. Drechsler, J.-M. Verbavatz, D. Touraud and W. Kunz, *J. Colloid Interface Sci.*, 2008, **319**, 542.
13 R. Abdel-Rahem, *Adv. Colloid Interface Sci.*, 2008, **141**, 24.
14 Kabir-ud-Din, Z. A. Khan and S. Kumar, *Colloid Polym. Sci.*, 2008, **286**, 335.
15 P. Baglion and L. Keran, *J. Phys. Chem.*, 1987, **91**, 1516.
16 M. Aamodt, M. Landgren and B. Jonsson, *J. Phys. Chem.*, 1992, **96**, 945.
17 P. Sudheesh, S. M. Nair and L. Sreejith, *Asian J. Appl. Sci.*, 2008, **1**, 246.
18 Kabir-ud-Din, Z. A. Khan and S. Kumar, *Colloid Polym. Sci.*, 2008, **286**, 335.
19 P. M. Lindemuth and G. L. Bertrand, *J. Phys. Chem.*, 1993, **97**, 7769.
20 R. Zana, *Adv. Colloid Interface Sci.*, 1995, **57**, l.
21 L. A. Moreira and A. Firoozabadi, *Langmuir*, 2009, **25**, 12101.
22 T. Sidim and G. Acar, *J. Surfactants Deterg.*, 2013, **16**, 60.
23 R. Zana, C. Picot and R. Duplessix, *J. Colloid Interface Sci.*, 1983, **93**, 43.
24 B. Michels and G. Waton, *J. Phys. Chem. B*, 2003, **107**, 1133.
25 E. Hirsch, S. Candau and R. Zana, *J. Colloid Interface Sci.*, 1984, **97**, 318.
26 R. Zana, S. Yiv, C. Strazielle and P. Lianos, *J. Colloid Interface Sci.*, 1981, **80**, 280.
27 K. C. Kuperkara, J. P. Matab and P. Bahadur, *Colloids Surf., A*, 2011, **380**, 60.
28 S. L. David, S. Kumar and Kabir-ud-Din, *J. Chem. Eng. Data*, 1997, **42**, 198.
29 S. Kumar, Z. A. Khan and Kabir-ud-Din, *J. Surfactants Deterg.*, 2002, **5**, 55.
30 C. Tanford, *The Hydrophobic Effect: Formation Of Micelle And Biological Membranes*, Wiley, New York, 1980.
31 N. Gul, S. Kumar, B. Ahmad, R. H. Khan and Kabir-ud-Din, *Colloids Surf., B*, 2006, **51**, 10.
32 Z. Yaseen, S. U. Rehman, M. Tabish and Kabir-ud-Din, *J. Mol. Liq.*, 2014, **97**, 322.
33 L. Sreejith, S. Parathakkat, S. M. Nair, S. Kumar, G. Varma, P. A. Hassan and Y. Talmon, *J. Phys. Chem. B*, 2011, **115**, 464.
34 H. Yin, Z. Zhou, J. Huang, R. Zheng and Y. Zhang, *Angew. Chem., Int. Ed.*, 2003, **42**, 2188.
35 T. S. Davies, A. M. Ketner and S. R. Raghavan, *J. Am. Chem. Soc.*, 2006, **128**, 6669.

 

36 B. Jeong, K. M. Lee, A. Gutowska and Y. H. H. An, *Biomacromolcules*, 2002, **3**, 865.
37 C. W. Kan, E. A. S. Doherty and A. E. Barron, *Electrophoresis*, 2003, **24**, 4161.
38 T. N. C. Dantas, V. C. Santanna, A. A. D. Neto, E. L. B. Neto and M. Moura, *Colloids Surf., A*, 2003, **225**, 129.
39 P. Mukerjee, *Solution Chemistry of Surfactants*, ed. K. L. Mittal, Plenum, New York, 1979, p. 153.
40 P. M. Lindemuth and G. L. Bertrand, *J. Phys. Chem.*, 1993, **97**, 7769.
41 Kabir-ud-Din, D. Bansal and S. Kumar, *Langmuir*, 1997, **13**, 5071.
42 H. H. Kohler and J. Stranad, *J. Phys. Chem.*, 1990, **94**, 7628.
43 A. Desai, D. Varade, J. Mata, V. Aswal and P. Bahadur, *Colloids Surf., A*, 2005, **259**, 111.
44 T. S. Davies, A. M. Ketner and S. R. Raghavan, *J. Am. Chem. Soc.*, 2006, **128**, 6669.
45 B. A. Schubert, E. W. Kaler and N. J. Wagner, *Langmuir*, 2003, **19**, 4079.
46 R. Zana and E. Waler, *Giant Micelles: Properties and Applications*, CRC Press, 2007.
47 J.-H. Lee, J. P. Gustin, T. Chen, G. F. Payne and S. R. Raghavan, *Langmuir*, 2005, **21**, 26.
48 Y. I. Gonzalez, H. Nakanishi, M. Stjerndahl and E. W. Kaler, *J. Phys. Chem. B*, 2005, **109**, 11675.
49 N. Akter, S. Radiman, F. Mohamed, I. A. Rahman and M. I. H. Reza, *Sci. Rep.*, 2011, **1**, 71.
50 S. R. Raghavan and E. W. Kaler, *Langmuir*, 2001, **17**, 300.
51 S. R. Raghavan, G. Fritz and E. W. Kaler, *Langmuir*, 2002, **18**, 3797.
52 M. E. Cates and S. J. Candau, *J. Phys.: Condens. Matter*, 1990, **2**, 6869.
53 F. Kern, F. Lequeux, R. Zana and S. J. Candau, *Langmuir*, 1994, **10**, 1714.
54 P. Koshy, V. K. Aswal, M. Venkatesh and P. A. Hassan, *J. Phys. Chem. B*, 2011, **115**, 10817.
55 H. Rehage and H. Hoffman, *Mol. Phys.*, 1991, **74**, 933.
56 R. Ganapathy and A. K. Sood, *Langmuir*, 2006, **22**, 11016.
57 N. A. Spenley, M. E. Cates and T. C. B. MacLeish, *Phys. Rev. Lett.*, 1993, **71**, 939.
58 R. Abdel-Rahem, M. Gradzielski and H. Hoffmann, *J. Colloid Interface Sci.*, 2005, **288**, 570.
59 M. Aratono, N. Onimaru, Y. Yoshikai, M. Shigehisa, I. Koga, K. Wongwailikhit, A. Ohta, T. Takiue, B. Lhoussaine, R. Strey, Y. Takata, M. Villeneuve and H. Matsubara, *J. Phys. Chem. B*, 2007, **111**, 107.
60 R. G. Shrestha, L. K. Shrestha, T. Matsunaga, M. Shibayama and K. Aramaki, *Langmuir*, 2011, **27**, 2229.
61 G. C. Kalur, B. D. Frounfelker, B. H. Cipriano, A. I. Norman and S. R. Raghavan, *Langmuir*, 2005, **21**, 10998.